1.6 Hydraulic Jumps, Bores, Rarefaction Waves and Long's Experiment.

One of the traditional difficulties in learning about hydraulics is reaching an understanding of why hydraulically controlled solutions arise and how they are established. Calculations of steady flows merely show the existence of hydraulically controlled solutions for special values of the governing parameters (e.g. B=2.5 in Figure 1.7) and this gives the impression that such a might be difficult to realize in nature. On the other hand, observations and laboratory experiments show that controlled, subcritical-to-supercritical solutions tend to prevail when topography is large. To aid the intuition, it often helps to consider how steady flows are established as the result of time-dependent adjustment from a simple initial state, or as the result of varying the upstream conditions. One of the most thoroughly studied adjustment problems is the experiment of Long (1953,1954,1972) in which an obstacle is towed through a laboratory tank containing a fluid initially at rest. The initial fluid depth d_o is constant and the obstacle is towed at a fixed speed v_0 until a translating steady state is achieved in the vicinity of the obstacle. For a frictionless system, the experiment is equivalent to the sudden introduction of an obstacle into a moving stream of depth and velocity d_0 and v_0 (Figure 1.6.1). This is the viewpoint we will use. The outcome depends crucially on the height h_m of the obstacle relative to a critical value h_c . The latter is simply the obstacle height associated with a hydraulically controlled *steady* state whose upstream depth and velocity are d_o and v_o. This is exactly the height that appears in (1.4.11) if Q/w is interpreted as $v_0 d_0$. A nondimensional form of this relation is

$$\frac{h_c}{d_0} = 1 - \frac{3}{2}F_0^{2/3} + \frac{F_0^2}{2} \qquad (1.6.1)$$

where $F_0 = \dfrac{v_0}{\left(gd_0\right)^{1/2}}$.

For $h_m<h_c$ the sudden appearance of the obstacle generates disturbances that propagate away from the obstacle and leave behind an uncontrolled steady solution, either completely supercritical or completely subcritical. When the initial state is subcritical $v_0<(gd_o)^{1/2}$ a subcritical steady state with a dip in the upper surface is established (Figure 1.6.1b). Note that the disturbances propagating away from the obstacle are *isolated* in the sense that they do not permanently alter the flow into which they are propagating. For supercritical initial flow and $h_m<h_c$ a supercritical steady state is established, this time with the two isolated disturbances propagating downstream.

When $h_m>h_c$ the situation is quite different. The obstacle now generates an upstream *bore*: a propagating wave consisting of an abrupt increase in depth. As shown in Figure 1.6.1(c or d) the upstream bore increases the depth from d_0 to d_1. In practice, the bore can vary from a nearly discontinuous, turbulent transition to a gradual, and perhaps oscillatory, change. The latter is called an *undular bore*. Here, we have simply represented the bore as a depth discontinuity. Downstream of the obstacle the adjustment is caused by a bore and a rarefaction wave. In some cases the downstream bore may become stationary on the down-slope of the obstacle forming a hydraulic jump (Figure 1.6.1c). Over the obstacle a hydraulically controlled steady state develops, with subcritical flow upstream, supercritical flow downstream (perhaps connected to a hydraulic jump) and with critical flow at the sill. Finally, if the obstacle height exceeds a second threshold height h_b ($>h_c$), complete blockage of the flow can occur, as shown in Figure 1.6.1d.

Long's experiments give a particular view of the concept of hydraulic control, one in which obstacle gains the ability to permanently alter the far field flow. When $h_m<h_c$ the long-term influence of the obstacle is local; when $h_m>h_c$ this influence is global. In the latter case, it is often said that the obstacle exerts *upstream influence (*even though the downstream flow is also altered). Another virtue of Long's experiment is that the final steady state can be predicted from the initial conditions. To do so, one must analyze the time-dependent flow that has developed long after the obstacle is introduced. That is, the transients must have moved away from the obstacle and developed into fully developed bores and/or rarefaction waves. The analysis makes use of *shock-joining* conditions linking the uniform flows on either side of the transients. The full solution to the adjustment problem will be presented in the next section; first we must develop a theory for shock joining.

Bores and hydraulic jumps are nonhydrostatic and often highly turbulent. They involve changes in the depth and velocity that take place over a distance of the order of the fluid depth. This distance is very short in the context of our long-wave model and we will therefore represent the transition as a discontinuity in d and v, away from which the pressure is hydrostatic and the velocity independent of depth. As an example, consider a hydraulic jump consisting of a stationary discontinuity between two steady flows (Figure 1.6.2). Let (d_u,v_u) and (d_d, v_d) denote the depth and velocity immediately upstream and downstream of the jump. In practice, one must measure these end-state values far enough away from the jump that the fluid is hydrostatic. Then it is immediately clear from mass conservation that

$$v_u d_u = v_d d_d. \tag{1.6.2}$$

Although the channel width w may vary with y, the assumed abrupt nature of the jump means that w is essentially the same on each side of the jump. Hense w does not enter the above mass balance.

A second matching condition can be obtained from the observation that no external forces in the y-direction act on the fluid at the discontinuity. In practice, there might be a frictional stress acting along the bottom or a pressure component in the y-direction resulting from a non-zero bottom slope, however the force arising from this stress will be negligible if the length of the shock is sufficiently short. Hence the difference in the pressure forces on either side of the jump must equal the change in the momentum flux of fluid entering and leaving the jump. Since the integral of the hydrostatic pressure p over the fluid depth is the total pressure force acting horizontally at a particular section is $\rho w g d^2/2$. Similarly, the total momentum flux across a particular section is $\rho w v^2 d$. Our momentum budget therefore requires

$$d_u v_u^2 + g d_u^2/2 = d_d v_d^2 + g d_d^2/2\,. \qquad (1.6.3)$$

The quantity $\rho w(d\,v^2 + gd^2\;/\;2)$ is sometimes called the *flow force* and (1.6.3) shows that it is conserved across a jump.

If the discontinuity translates steadily at speed c_1, the above analysis can be repeated in a frame of reference moving with the discontinuity. Since the flow appears steady in this frame, and since the governing equations are invariant with respect to steady translation, (1.6.2) and (1.6.3) are again obtained, but with v_d and v_u interpreted as moving frame velocities. To return to the rest frame replace these velocities by v_d-c_1 and v_u-c_1, where v_d and v_u now denote the rest-frame velocities. The general shock joining relations are therefore given by:

$$(v_u - c_1)d_u = (v_d - c_1)d_d \qquad (1.6.4)$$

and

$$d_u(v_u - c_1)^2 + g d_u^2/2 = d_d(v_d - c_1)^2 + g d_d^2/2 \qquad (1.6.5)$$

If the end states are unsteady, the shock speed will vary with time. In this case it is possible to show that (1.6.4) and (1.6.5) continue to hold, but we leave the proof as an exercise for the reader.

Equations (1.6.2) and (1.6.3) allow the downstream state of a hydraulic jump to be calculated given a known upstream depth and velocity. These relations also show that energy is not conserved crossing the jump. Since $B_u = \frac{v_u^2}{2} + g d_u$ is the energy per unit mass of any fluid element entering the jump, the total energy influx is QB_u and the total outflux is QB_d. The difference between these two is proportional to the rate of energy dissipation $-\dot{E}$ (per unit mass) within the jump. Using (1.6.2) and (1.6.3) it can be shown that

$$-\dot{E} = \frac{gQ}{4}\frac{(d_d - d_u)^3}{d_d d_u} \qquad (1.6.6)$$

Energy dissipation requires the downstream depth to exceed the upstream depth, ‘downstream’ meaning the direction of positive Q. For a bore, the above expression is valid if Q is interpreted as $(v_u - c_1)d_u w$, the transport in the moving frame of the bore. Thus, the depth of fluid passing through the bore must increase in order for energy to be dissipated. It is remarkable that $\dot{E}$ can be calculated independently of viscosity or even the form of internal dissipation.

Since a bore or jump contains no internal sources of energy, the fluid depth must increase in the direction of flow passing through. This is an important constraint as (1.6.4) and (1.6.5) admit solutions with positive *and* negative dissipation. An example can be found though elimination of c_1-v_d from (1.6.4) and (1.6.5), yielding

$$\left(c_1 - v_u\right)^2 = gd_d\left(\frac{d_d + d_u}{2d_u}\right). \qquad (1.6.7)$$

The left-hand side of this relation is the speed of a bore relative to the velocity of the fluid to the left . For given v_u, d_d, and d_u, two solutions for c_1 can be found corresponding to the positive and negative square roots of the right-hand side. The positive root corresponds to fluid entering the bore from the right while the negative root corresponds to fluid entering from the left. If $d_d > d_u$ the negative root must be selected.

Returning temporarily to the case of a stationary jump, a bit of manipulation of (1.6.2) and (1.6.3) leads to

$$\frac{d_d}{d_u} = \frac{-1 + \sqrt{1 + 8F_u^2}}{2} \qquad (1.6.8)$$

where $F_u = v_u / \sqrt{gd_u}$, the Froude number of the approach flow. Since the fluid depth must increase in the direction of the flow, $d_d/d_u > 1$ and thus F_u must exceed unity. The approach flow must be supercritical. Since the subscripts u and d can be interchanged without effecting (1.6.2) and (1.6.3), an expression involving the downstream Froude number $F_d = v_d / \sqrt{gd_d}$ can be obtained simply by interchanging the subscripts in (1.6.8). Thus

$$\frac{d_u}{d_d} = \frac{-1 + \sqrt{1 + 8F_d^2}}{2}, \qquad (1.6.9)$$

showing that the downstream flow must be subcritical. In summary, the bore overtakes linear waves propagating against the upstream flow but is overtaken from the rear by the same type of linear waves. The convergence of waves at the discontinuity, which is an extension of the steepening process discussed earlier, is instrumental in maintaining the bore.

The hydraulic jump provides a mechanism for a supercritical flow to join to a downstream subcritical flow with the same Q but lower B. For the steady solutions sketched in Figure 1.7, this means that the hydraulically controlled flow ($\tilde{B}$=5/2) could connect to one of the solutions for which $\tilde{B}$<5/2. The connection would occur in the form of a hydraulic jump on the down-slope of the obstacle, and one possibility is indicated in the figure.

The above analysis takes for granted that the jump or bore occurs over a horizontal distance short enough that bottom friction and other external sources or sinks of momentum are insignificant. For hydraulic jumps this assumption is valid as long as the Froude number of the approach flow is greater than about 1.7 (Chow, 1965). Then the depth change occurs over a horizontal distance on the order of the fluid depth. Such a change is tantamount to a discontinuity in the gradually varying framework of shallow-water dynamics. For Froude numbers <1.7 however, the jump becomes undular (wavelike) and the depth changes occur over a much longer distance. Non-hydrostatic effects are essential to the wavy structure of the jump and the increased horizontal length may necessitate consideration of additional sources of momentum. The reader is referred to Baines (1995) for a discussion.

Some of the best places to observe bores are over gently sloping beaches such as those of southern California (Figure 1.6.3). On the left-hand side of the photo is a turbulent bore caused by the shallow surge of a wave running towards the beach. The middle of the photo shows a fairly quiescent, V-shaped region in which the water depth is just a few inches. To the right is the smooth, wavy front of a surge that is running away from the beach. The latter was generated by a previous wave that ran up on the beach and is now spilling back. This reverse surge is a good example of an undular bore.

Discontinuities, real or contrived, are encountered quite often in fluid dynamics. In many situations, matching conditions are found by integration across the discontinuity of the equations governing the flow away from it. Of course, this procedure is only valid when the governing equations hold at the discontinuity as well. One must take great care in applying this method to free-surface jumps and bores, for which the shallow water equations do not hold. For example, (1.6.5) cannot be derived by integrating the shallow water momentum equation (1.2.1) across the discontinuity. Doing so would lead to the conclusion that the Bernoulli function B is conserved across the shock, which clearly incorrect . A valid procedure in this case is to apply a more primitive version of the y-momentum equation such as

$$\frac{d}{dt}\iiint_V \rho v \; dxdydz = \sum_{\partial V} F^{(y)}\,, \qquad (1.6.10)$$

which is valid throughout the fluid. Here V is any material volume in the fluid and the right hand side of (1.6.10) is the sum of forces $F^{(y)}$ in the y-direction around the bounding surface ∂V. If the shallow water approximations for v and $F^{(y)}$ are substituted directly into (1.6.10) the result is the so called *flux* form of the y-momentum equation:

$$\frac{\partial(vd)}{\partial t} + \frac{\partial}{\partial y}\left[v^2 d + gd^2/2\right] = 0\,, \qquad (1.6.11)$$

which can also be obtained by multiplying (1.2.1) by d and using the continuity equation (1.2.2). Although it is formally invalid within the jump, (1.6.11) yields the correct matching condition when integrated across a discontinuity in depth. Numerical solutions of the shallow water equations based on the finite-difference method frequently use (1.6.11) in place of (1.2.1) since the resulting solutions obey the correct matching conditions when jumps and bores are present. *(We may write a section on numerical methods and, if so, should inform the reader where this will be.)*

The above discussion has assumed a single layer flow with a free upper surface, but most ocean and atmospheric applications will involve an overlying or underlying fluid slightly different density. Experiments by Wilkinson and Wood (1971) reveal the anatomy of such a jump when the second fluid is relatively deep and inactive (Figure 1.6.4). The jump consists of two stages, an upstream region in which overlying fluid is entrained down into the moving layer, and a 'roller' region with a large anticyclonic eddy. The Froude number based on reduced gravity remains <1 in the entrainment region and jump to below unity downstream of the roller. Entrainment is produced by shear instabilities at the interface between the two fluids. At the top of the roller, where the velocity is negative and the vertical shear is reduced relative to upstream values, entrainment is not observed. By traditional definition the entrainment region and the roller comprise the hydraulic jump, even though the entraining region may be quite long compared to the roller.

The presence of entrainment gives rise to a significant departure from the single-layer case considered earlier. One of the consequences is that for a given upstream state there is no unique downstream state. As demonstrated by Wilkinson and Wood a range of downstream states may be found by varying the height h_m of an obstacle placed downstream of the jump (Figure 1.6.4). Lowering h_m causes the roller region to migrate downstream, lengthening the entraining regions and increasing the total amount of entrainment. For sufficiently small h_m the roller disappears and the jump consists entirely of a gradually deepening region of entrainment. This is the state of maximum entrainment. If h_m is increased, the roller moves upstream and eats up the entrainment region. For sufficiently large h_m the entrainment region disappears and the jump consists only of the roller. An further increase in h_m causes the roller to come into contact with the vertical wall beneath which lower layer fluid is injected. The jump at this point is said to be flooded. Photographs of the three cases (no roller, combination of entrainment region and roller, and flooded jump) are shown (Figure 1.6.5) for the Wilkinson and Wood experiment, an upside-down version of the scheme we have been discussing.

Entrainment gives rise to a lack of conservation of mass and volume flux in the lower layer. If E is the volume flux per unit width introduced into the lower layer by entrainment, then mass and volume flux balances for the lower layer between sections immediately upstream and downstream of the jump (Figure 1.6.5) are

$$v_u d_u + E = v_d d_d \qquad (1.6.12)$$

and

$$\rho_{2u} v_u d_u + E\rho_2 = \rho_{2d} v_d d_d \,.$$

Subtracting the product of ρ_2 and the first equation from the second leads to

$$(\rho_{2u} - \rho_1) v_u d_u = (\rho_{2d} - \rho_1) v_d d_d \,,$$

which is often written in form

$$g'_u v_u d_u = g'_d v_d d_d \, , \qquad (1.6.13)$$

where $g'_0 = g(\rho_{20} - \rho_1)/\rho_1$. The quantity $g'vd$ is called *buoyancy flux* and its conservation is a consequence of the total conservation of mass for the two layers as a whole.

Further complicating the problem of shock joining is that fact that a horizontal pressure force, exerted by the overlying fluid, now exists on the upstream face of the roller and the top of the entraining region. However, the flow force for the two layers as a whole remains conserved provided the bottom is horizontal and frictional bottom drag is negligible. To find the total flow force, we assume that the upper layer is motionless, implying that the free surface (z=D) is level. Integrating the hydrostatic pressure over the whole depth of the layer then leads to

$$g\rho_1 \frac{D^2}{2} + g(\rho_{2u} - \rho_1)\frac{d_u{}^2}{2} + d_u v_u{}^2 = g\rho_1 \frac{D^2}{2} + g(\rho_{2d} - \rho_1)\frac{d_d{}^2}{2} + d_d v_d{}^2 \qquad (1.6.14).$$

The first term on each side of the equation is the barotropic pressure force, equal to the force that would exist if the fluid had uniform density ρ_1. The second term is the extra pressure force due to the excess density of the lower layer. Cancel the barotropic term and one is left with an expression identical in form to the case of a single layer (*cf.* 1.6.3).

If the entrainment E is known, then (1.6.12-1.6.14) provide three relations for the downstream velocity, layer depth, and density can be calculated from upstream values. Of course E is not known in advance nor, as shown by the experiment, can it be predicted solely on the basis of the upstream state. Some sort of downstream information, or an assumption about the downstream flow, must be made. An approach taken by Wilkinson and Wood (1971) is to assume that the downstream flow is hydraulically controlled by an obstacle of height h_m, as in the experiment. It is further assumed that no entrainment or dissipation occurs between the downstream section x_d and the sill. Although two additional unknowns (the velocity and layer thickness at the sill) are introduced, there are three constraints. These include conservation of energy and volume flux as well as the critical condition at the sill. For given h_m the entrainment can be calculated and the problem closes.

Although this last procedure is elegant, it is difficult to apply in geophysical settings due to the general lack of a clearly defined downstream obstacle or h_m value. Supercritical flows often spill out onto vast terrestrial or abyssal plains and the factors controlling the downstream layer thickness are complex. Alternatives to the Wilkinson and Wood procedure use turbulence closure assumptions to predict the energy dissipation or entrainment in the jump. The reader is referred to the work by Qinfang and Smith (2001a,b), Holland et al. (2002) and references contained therein. *Also could refer to a more recent paper I have reviewed, provided that it appears.*

Exercises

1) Derive the shock joining conditions for a hydraulic jump in a channel with the same triangular cross-section as that given in problem 4 of Section 1.4.

2) Consider a bore propagating in a flow with spatially and temporally varying velocity and depth. The speed of the bore is unsteady: $c_1=c_1(t)$. Define a material volume V bounded by the free surface, the side walls of the channel, and by material fluid columns located at position $a(t)<y<b(t)$ as shown in Figure 1.6.2. Also, let y_u and y_d be fixed positions lying within the volume as shown in the figure.

(a) Show that

$$\frac{d}{dt}\iiint_V v\ dxdydz = w\left[\frac{d}{dt}\int_{a(t)}^{y_u}(dv)dy + \frac{d}{dt}\int_{y_u}^{y_d}(dv)\ dy + \frac{d}{dt}\int_{y_d}^{b(t)}(dv)dy\right]$$

(b) Note that the above equation also applies in a steadily translating frame of reference. Let the speed of translation be $c_1(0)$, so that the frame speed matches the bore speed at $t=0$. By shrinking the distances between $a(t)$, y_u, y_d, and $b(t)$ to zero , show that at $t=0$

$$\frac{d}{dt}\int_{a(t)}^{y_u}(dv)dy \to -v_u^2 d_u$$

$$\frac{d}{dt}\int_{y_u}^{y_d}(dv)\ dy \to 0$$

$$\frac{d}{dt}\int_{y_d}^{b(t)}(dv)dy \to v_d^2 d_d$$

where $v_u=(\ da/dt)_{t=0}$ and $v_d=(db/dt)_{t=0}$.

(c) By applying (1.6.10) and evaluating the forcing terms on the right-hand side using the hydrostatic pressure at $y=a(0)$ and $y=b(0)$, show that (1.6.3) is recovered. Note that (1.6.5) follows by transformation back to a rest frame.

(d) Perform the same series of operations starting with a primitive statement of mass conservation in order to recover (1.6.4) for an unsteady shock.

Figure Captions

1.6.1 Schematic depiction of the various types of shallow-water adjustment caused when an obstacle is introduced into a uniform, subcritical stream (a). In (b) the obstacle height is less than the critical value and the flow remains subcritical. In (c) the obstacle exceeds its critical height and a hydraulically controlled flow with a jump emerges. In such cases the jump may also propagate downstream as a bore. In (d) the obstacle has exceeded the height required for complete blocking. (The downstream disturbances are not shown for this case.)

1.6.2 An abstraction of a hydraulic jump.

1.6.3 The foamy wave front is a bore, formed by the leading edge of a wave propagating onto a gently sloping beach in southern California. The wavy feature to the right is an undular bore that is propagating in the opposite direction (right-to-left). The latter is formed at the leading edge of a long wave that has been reflected from the beach. (L. Pratt photo.)

1.6.4. A schematic view of the two-fluid jump observed by Wilkinson and Wood (1971).

1.6.5 Photographs of the laboratory experiment of Wilkinson and Woods (1971).

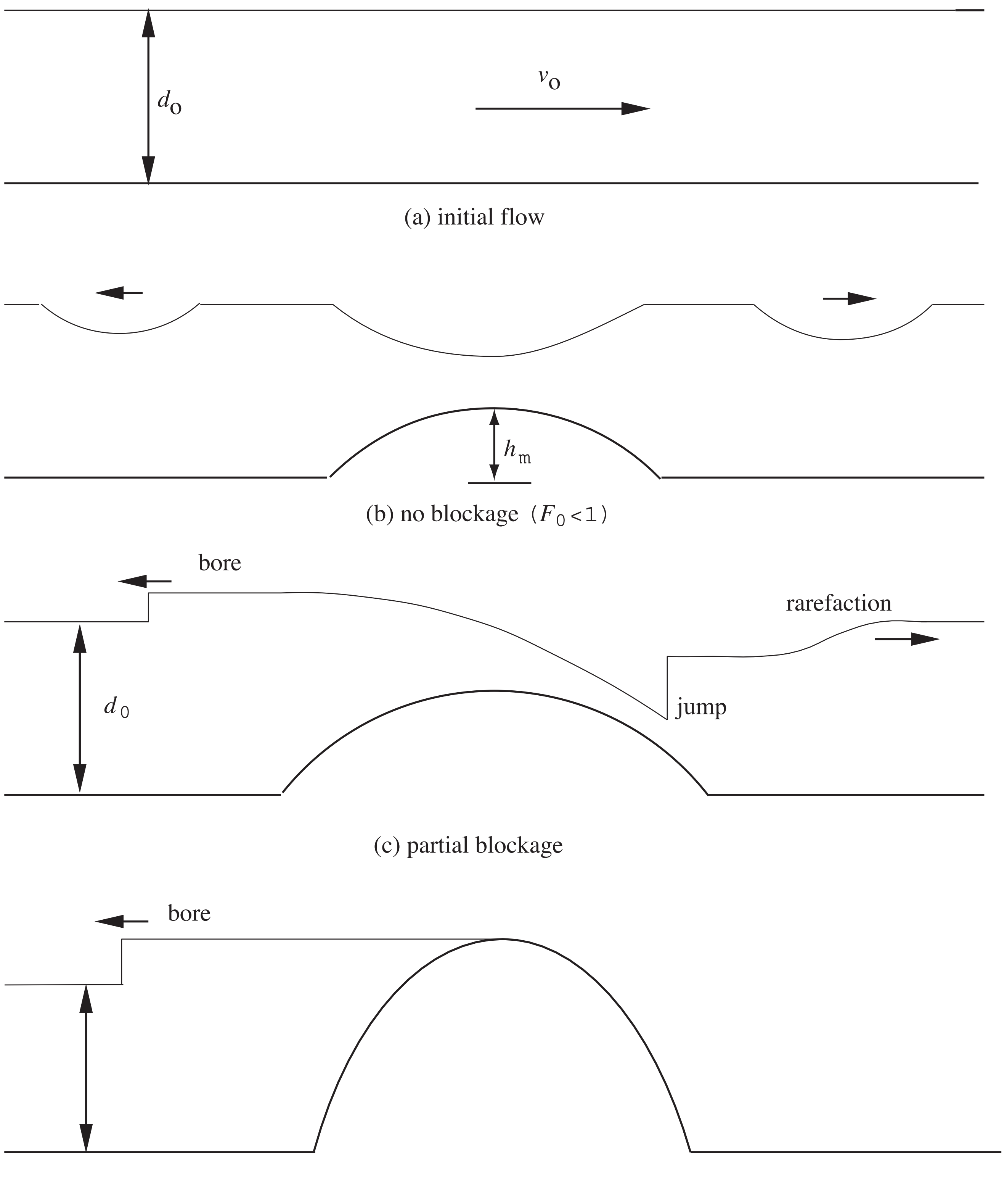

d_o
v_o
(a) initial flow
h_m
(b) no blockage (F_0<1)
bore
rarefaction
d_0
jump
(c) partial blockage
bore
(d) total blockage

Figure 1.6.1

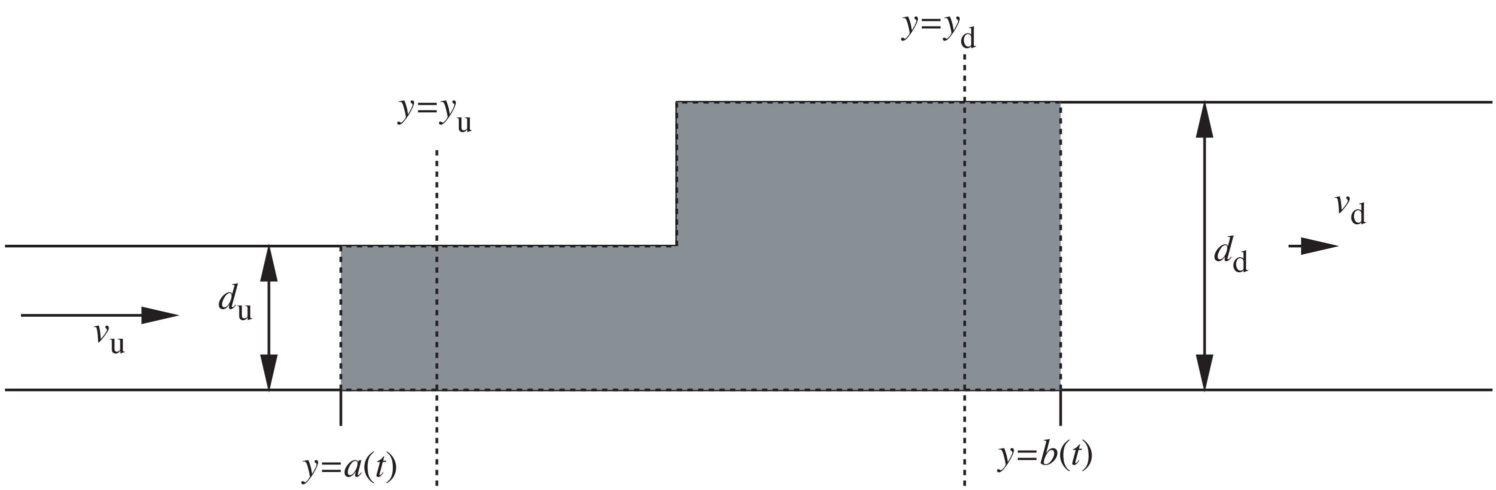

Figure 1.6.2

Figure 1.6.3

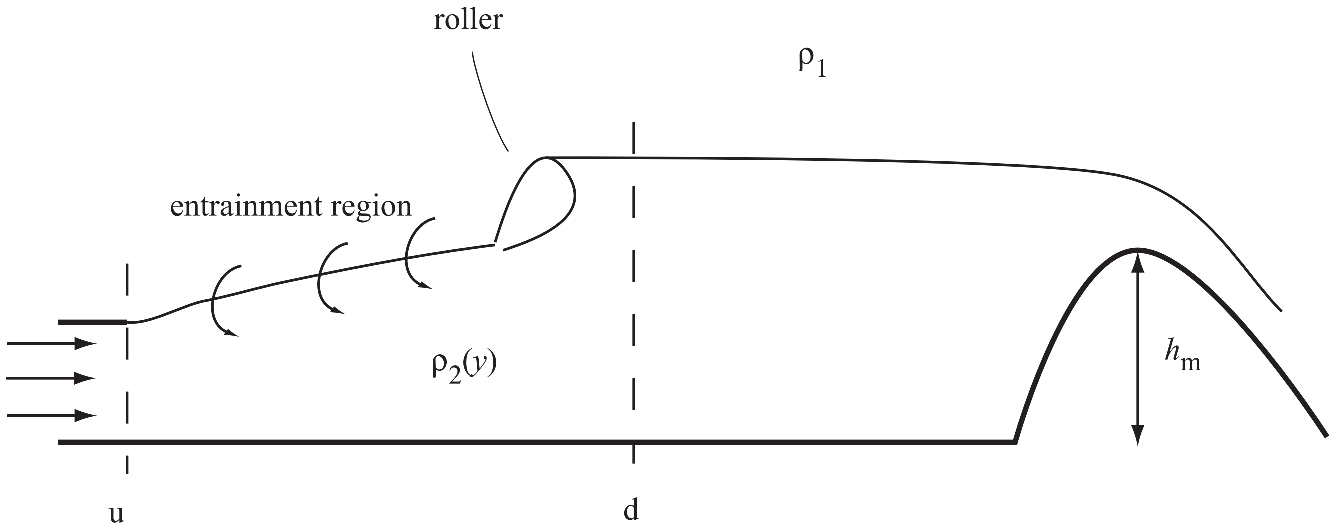

Figure 1.6.4

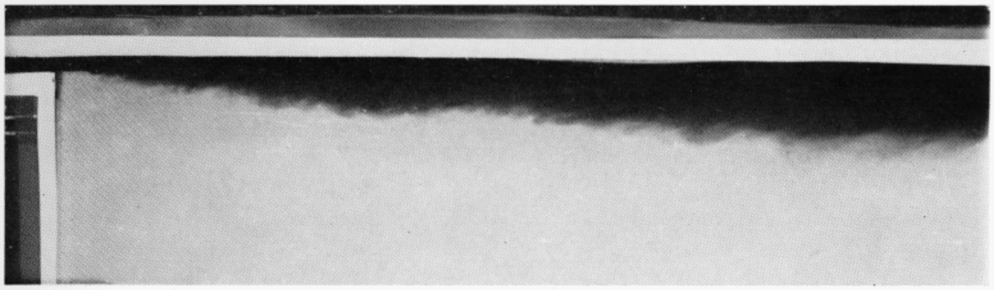

A density jump of the maximum entraining type with a free overfall downstream. Entrainment is occurring along the length of the jump.

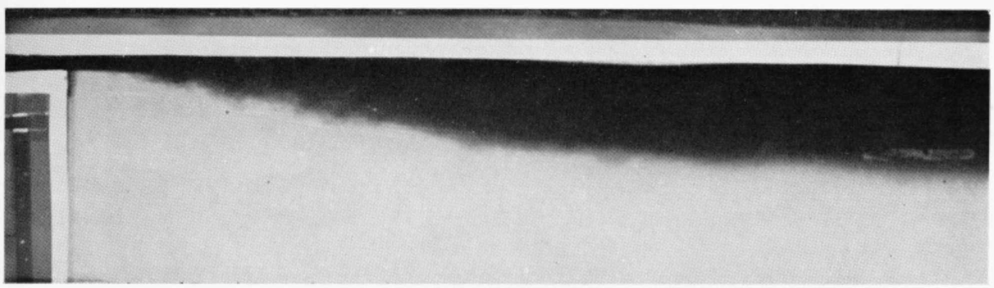

. A density jump controlled by a broad crested weir downstream. Entrainment is occurring only at the far upstream end of the jump, the remainder consists of a roller zone.

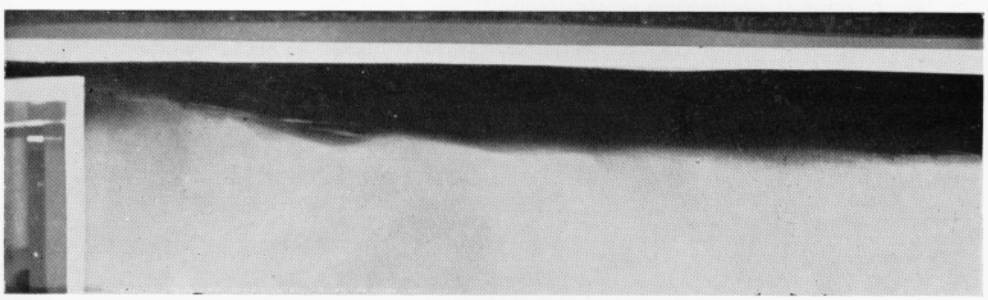

Photograph of a flooded density jump. The inlet flow for this jump is identical to that of the jumps shown in figures 1 and 2.

Figure 1.6.5